

Modification of transparent and conducting single wall carbon nanotube thin films via bromine functionalization

Giovanni Fanchini,^{a)} Husnu Emrah Unalan, and Manish Chhowalla
Materials Science and Engineering, Rutgers University, Piscataway, New Jersey 08854

(Received 1 October 2006; accepted 23 January 2007; published online 1 March 2007)

The results of bromine doping of transparent and conducting single wall carbon nanotube (SWNT) thin films are described. Br profoundly effects the density of states (DOS) of SWNTs which leads to dramatic improvement in the electrical properties. The authors show that the role of the Br is not only in shifting the Fermi level but also in forming acceptor sites in metallic SWNTs. These modifications of the DOS through bromination lead to simultaneous increase in both the on/off ratio and mobility of thin film transistors. Furthermore, the transistor characteristics of Br-functionalized SWNTs are similar in air, inert atmosphere, and vacuum. © 2007 American Institute of Physics.

[DOI: 10.1063/1.2709903]

Presently there is an effort underway to optimize the performance of thin films from low density networks of single wall carbon nanotubes (SWNTs) because they can be transparent, semiconducting, and flexible.¹⁻⁹ The uniform deposition of SWNT networks²⁻⁵ has led to thin films with conductance values greater than $5 \times 10^{-4} \Omega^{-1} \cdot \square$ and transparency above 90%.¹ The main limitation of the devices is the presence of metallic SWNTs in the network which enhances the mobility but leads to a high current in the off state which reduces the on/off ratio. Several methods have been reported to separate the semiconducting SWNTs from metallic ones with limited success.¹⁰⁻¹² Another approach to separation is to modify the electronic structure of the SWNTs through functionalization with specific molecules or atoms.¹³⁻¹⁵ Recently, preparation of mostly semiconducting SWNTs has been reported using nitronium ions.¹⁶ In addition to nitronium ions, physisorbed bromine, iodine, and diazonium salts have been used to modify the electronic density of states of SWNTs. In this letter, we report chemical functionalization of transparent and conducting SWNT thin films with bromine which leads to dramatic changes in the electrical properties of the SWNTs.

The chemical attachment of Br to the SWNTs was performed on carboxylated SWNTs. It has been known for a long time that graphite can be partially etched by Brodie's reagent,¹⁷ a mixture of azeotropic nitric acid and potassium chlorate (KClO₃), which produces a residual by-product called graphitic acid, a mixture of graphitic islands decorated by COOH groups. We explored the effects of Brodie's reagent on SWNTs at different KClO₃:SWNT ratios and found 0.75 in weight fraction to be the ideal composition. After etching with Brodie's agent, the recovered SWNTs were treated with phosphorus tribromide (PBr₃) in order to obtain chemically bonded Br functionalized SWNTs. Our process of exposing the SWNTs to acyl bromide functional groups is analogous to the acyl chloride process described by Chen *et al.*¹⁸ The Br reaction was monitored by means of measuring the decrease in pH due to the released phosphoric acid.

The SWNT thin films were deposited using the vacuum filtration process.³ The membranes were etched in repeated tetrahydrofuran baths followed by washing in chloroform.

The Br content was determined by x-ray fluorescence (XRF) spectra by means of the Sherman equation¹⁹ and a KBr calibration sample. We found that the SWNTs contain approximately one Br atom per 20 C sites when functionalized at KClO₃:SWNT=0.75. This relatively high amount of Br content can only be accounted for if sidewall functionalization of the SWNTs has occurred. Infrared (IR) spectra (not shown here) revealed peaks at 500–700, 1000–1100, and 1600 cm⁻¹, which are consistent with C–Br, activated C–C, and C=O bond stretching vibrations in C–COBr groups.²⁰

The scanning electron microscopy (SEM) images of the brominated SWNT thin films deposited at three different concentrations are shown in Fig. 1. The SWNT density on the surface is observed to increase with nanotube concentration in the suspension, as expected. The Raman spectra of purified but undoped and Br doped SWNT thin films are shown in Fig. 2. The absence of significant *D*-peak broadening and the presence of Raman radial breathing modes after functionalization demonstrate that the skeleton of the SWNTs remains undamaged during the process. The changes in intensity and peak position of the Raman radial breathing modes along with up shift in Raman *G* peak (from 1592 to 1605 cm⁻¹) recorded at 514.5 nm excitation indicate that the electronic structure of the SWNTs has undergone a dramatic change after Br functionalization.¹⁴ Furthermore, it can be seen that the metallic feature in the *G* peak is suppressed in the Br doped SWNT sample compared to the undoped one.

The sheet conductivity (σ) versus the relative nanotube fraction (Φ) for Br doped and undoped SWNT thin films is plotted in Fig. 2(b). The trend of the nonbrominated films can be fitted by the expression

$$\sigma = \sigma_0(\Phi - \Phi_c)^n, \quad (1)$$

which is typical of network of sticks above the percolation threshold (Φ_c). We observe from Fig. 2(b) that, any given fraction (Φ) of SWNTs, the Br doped SWNT films sit above the line determined by Eq. (1). Also such increase in conductivity can be understood within the percolation theory. Indeed Eq. (1) can be adapted to describe the conductivity of brominated films by replacing $\sigma_0 = 1.1 \Omega^{-1} \cdot \square$, with $\sigma_{\text{Br}} = 8.0 \Omega^{-1} \cdot \square > \sigma_0$. Since the prefactor in Eq. (1) is related to the conductivity of the single stick in the percolating

^{a)}Electronic mail: fanchini@rci.rutgers.edu

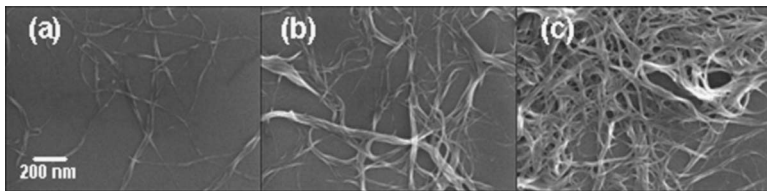


FIG. 1. (Color online) (a) SEM images of SWNT thin films at concentrations of (a) 0.5 ml/g, (b) 1 mg/l, and (c) 2 mg/l. The filtration volume was kept constant at 50 ml.

network, this shows that the conductivity of the individual Br doped tube is higher.

We also performed spectroscopic ellipsometry in order to gain insight into the density of states (DOS) of Br doped SWNT thin films. The complex refractive index of the Br doped SWNT thin films is shown in Fig. 2(c). Both the real and imaginary parts of the complex dielectric function exhibit a small but distinct feature at photon energy, $E_{\text{Br}-\pi^*} = 2.9$ eV, which is not present in nonbrominated samples prepared at the same SWNT density. The presence of this peak indicates the creation of additional electronic states in the brominated SWNTs. In order to investigate the significance of this peak and reconcile the increase in semiconducting character predicted by Raman with conductivity increase, we performed *ab initio* density functional theory simulations using local spin density approximation for the exchange-correlation term.²¹ 180 k points were used along the tube axis to determine the DOS. Simulations were carried on (11,0) and (12,0) undoped SWNTs and unrelaxed SWNTs with sidewalls functionalized by acyl bromide (COBr) groups, in agreement with the IR results. The C:Br ratio in simulated nanotubes was 20:1.

The simulated DOS of the undoped and Br doped metallic (12,0) SWNT are shown in Fig. 3(a). In metallic SWNTs, three main effects related to the attachment of Br are found from calculations: (i) the downshift of the Fermi level toward the valence band due to draining of electrons toward the highly electronegative Br sites, (ii) the appearance in both semiconducting and metallic SWNTs of a Br-related acceptor peak above the Fermi level, and (iii) a significant decrease of the DOS at the midgap in metallic SWNTs. These effects are schematically indicated in Fig. 3(b). Thus, from these simulation results we assign the Br-related peaks observed in ellipsometry at 2.9 eV to $p \rightarrow \pi^*$ electronic transitions between the low-energy acceptor states (p) near the Fermi level and the π^* DOS band of the SWNT network. This allows us to reconstruct the DOS

and the optical transitions occurring in our Br-doped films, as shown in Fig. 3(b).

Thus, based on our simulations results we can reconcile the decrease in the metallic character found in Raman and the increase in the sheet conductivity for brominated SWNT thin films in the following manner. First, since Br is a highly electronegative element, it effectively localizes free electrons in the metallic SWNTs so that a small energy barrier is required for delocalization. This phenomenon essentially changes the character of metallic SWNTs into semimetallic, suppressing the Fano resonance feature in the Raman spectrum, as shown in Fig. 2. Second, the additional states introduced near the Fermi level do not directly contribute to the overall conductivity but rather they behave as acceptor levels. Therefore, the movement of the Fermi level toward the valence band increases the amount of holes at the band edge, leading to a transport mechanism comparable to that of a doped semiconductor.

Thin film transistors (TFT) characteristics from undoped and Br-doped SWNTs are shown in Figs. 4(a) and 4(b), respectively. The mobility and on/off ratio of the devices from undoped SWNTs were $0.04 \text{ cm}^2/\text{V s}$ and 15, respectively. Our transistor characteristics are somewhat lower than those reported in the literature which could be attributed to bundling of SWNTs during the filtration process. However, devices from Br doped SWNTs show a significant improvement in the mobility ($\mu \approx 5 \text{ cm}^2/\text{V s}$) and on/off ratio (200). We observe that Br functionalization allows the fabrication of devices with thin films deposited at much higher SWNT density. It is generally accepted¹ that the performance of dense SWNT TFTs is limited above a critical density by the percolation threshold of the metallic SWNTs. That is, high on/off ratios generally result in mobility values of typically around $0.1\text{--}1 \text{ cm}^2/\text{V s}$, while high mobility values result in devices with on/off ratios of around 10–100.

Thus, our results indicate that Br attachment eliminates the limitations of previous SWNT thin film transistors be-

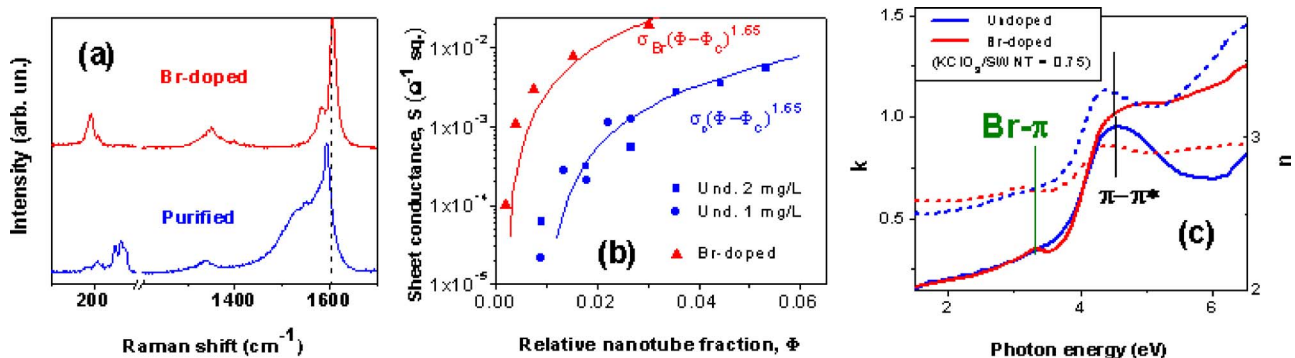


FIG. 2. (Color online) (a) Raman spectra of doped and fully Br doped SWNT thin films. The Fano resonance peak is significantly diminished in the Br doped films in comparison to the undoped material. (b) Sheet conductivity vs the relative SWNT fraction. The conductivity of the Br doped thin films has been substantially improved and the mechanism deviates from the percolation relationship followed by the undoped samples as indicated by the lines. (c) Complex dielectric function of doped and undoped samples measured using spectroscopic ellipsometry showing the acceptor peak at 2.9 eV in bromine doped SWNTs. Downloaded 12 Mar 2007 to 128.6.227.182. Redistribution subject to AIP license or copyright, see <http://apl.aip.org/apl/copyright.jsp>

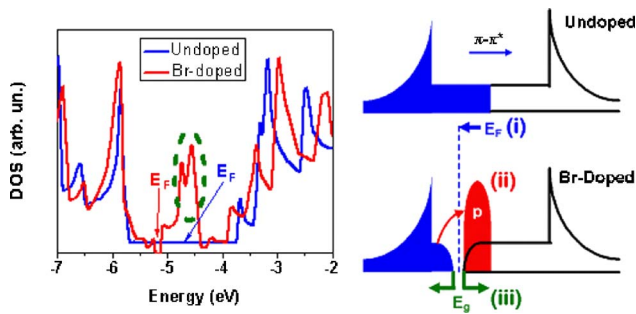


FIG. 3. (Color online) Results of the LDA simulations on undoped and sidewall-functionalized (12,0) metallic SWNT. (a) The density of states of undoped and Br doped samples showing the downshift in Fermi level, appearance of the acceptor peak, and the reduction of states at the Fermi level. The right panel shows the schematic representation of the findings. The top schematic shows the undoped case, while the bottom shows the three effects deduced from simulations.

cause the amount of extended electronic states in the metallic SWNTs is strongly depleted. Furthermore, the downshift of the Fermi level and the presence of acceptor states just above such a level facilitate the formation of holes in the valence band at finite temperature. We therefore conclude that, in Br doped thin films, the electrons in metallic SWNTs are not only confined but they are also reactivated by bromine, since they actually behave as *p*-type semimetallic elements. More importantly, the depletion of midgap electron states allows the fabrication of transistors at higher SWNT density which in turn increases the mobility without lowering the on/off ratio. We also argue that our device characteristics could be further improved through better dispersion of our SWNTs.

Physisorbed bromine doping is recognized as highly unstable. We argue that our functionalization method is more

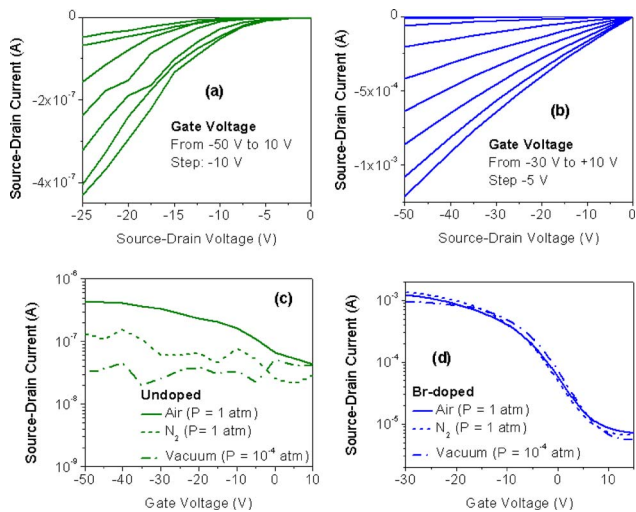


FIG. 4. (Color online) Optimized transistor characteristics on devices fabricated from (a) undoped SWNTs and (b) Br doped SWNTs. Gate scan of transistors from (c) undoped and (d) Br doped SWNTs recorded in air, in vacuum, and in inert atmosphere (N_2). The devices were kept in the measuring environment for 1 h before performing the measurements in vacuum and in N_2 .

stable because the Br is chemically attached to the SWNTs. In order to verify this, we have investigated the stability of our Br functionalized devices by measuring their performance in different atmospheres. Figures 4(c) and 4(d) compare the gate scans of the undoped and Br doped devices, respectively. In contrast to devices from purified SWNTs, no clear environmental effect is detectable in Br doped transistors indicating that these devices are stable.

In conclusion, we have described how attachment of Br to SWNTs leads to profound changes in the electrical properties of transparent and conducting SWNT thin films. We show that the increase in conductivity and the decrease in the metallic character from Raman in the brominated SWNT thin films can be reconciled through the appearance of acceptor peak and a decrease in the DOS at the Fermi level. The TFTs fabricated from Br doped SWNTs performed better in terms of mobility and on/off ratio due to the suppression of metallic nanotubes. Furthermore, chemical bonding of Br to SWNTs allows the fabrication of stable devices, in contrast to undoped devices which unstable in vacuum and nitrogen due to the evolution of physisorbed oxygen.

¹L. Hu, D. S. Hecht, and G. Gruner, *Nano Lett.* **4**, 2513 (2004).

²A. Du Pasquier, H. E. Unalan, A. Kanwal, S. Miller, and M. Chowalla, *Appl. Phys. Lett.* **87**, 203511 (2005).

³H. E. Unalan, G. Fanchini, A. Kanwal, A. Du Pasquier, and M. Chowalla, *Nano Lett.* **6**, 677 (2006).

⁴Z. Wu, Z. Chen, X. Du, J. M. Logan, J. Sippel, M. Nikolou, K. Kamaras, J. R. Reynolds, D. B. Tanner, A. F. Hebard, and A. G. Rinzler, *Science* **305**, 1273 (2004).

⁵E. Artukovic, M. Kaempgen, D. S. Hecht, S. Roth, and G. Gruner, *Nano Lett.* **5**, 757 (2005).

⁶*Carbon Nanotubes: Synthesis, Structure, Properties and Applications*, Topics in Applied Physics Vol. 80, edited by M. S. Dresselhaus, G. Dresselhaus, and P. Avouris (Springer, New York, 2001), pp. 113–146.

⁷R. Seidel, A. P. Graham, E. Unger, G. S. Duesberg, M. Liebau, W. Steinhögl, F. Kreupl, W. Hoenlein, and W. Pompe, *Nano Lett.* **4**, 831 (2004).

⁸T. Durkop, S. A. Getty, E. Cobas, and M. S. Fuhrer, *Nano Lett.* **4**, 35 (2004).

⁹D. E. Johnston, M. F. Islam, A. G. Yodh, and A. T. Johnson, *Nat. Mater.* **4**, 589 (2005).

¹⁰R. Krupke, F. Hennrich, H. V. Lohneysen, and M. M. Kappes, *Science* **301**, 344 (2003).

¹¹D. Chattopadhyay, I. Galeska, and F. Papadimitrakopoulos, *J. Am. Chem. Soc.* **125**, 3370 (2003).

¹²M. Zheng, A. Jagota, E. D. Semke, B. A. Diner, R. S. Mclean, S. R. Lustig, R. E. Richardson, and N. G. Tassi, *Nat. Mater.* **2**, 338 (2003).

¹³M. Shim, J. H. Back, T. Onzel, and K. W. Kwon, *Phys. Rev. B* **71**, 205411 (2005).

¹⁴A. M. Rao, P. C. Eklund, S. Bandow, A. Thess, and R. E. Smalley, *Nature (London)* **388**, 257 (1997).

¹⁵R. S. Lee, H. J. Kim, J. E. Fischer, A. Thess, and R. E. Smalley, *Nature (London)* **388**, 255 (1997).

¹⁶K. H. An, J. S. Park, C. M. Yang, S. Y. Jeong, S. C. Lim, C. Kang, J. H. Son, M. S. Jeong, and Y. H. Lee, *J. Am. Chem. Soc.* **127**, 5196 (2005).

¹⁷B. C. Brodie, *Philos. Trans. R. Soc. London* **149**, 249 (1859).

¹⁸J. Chen, M. A. Hamon, H. Hu, Y. Chen, A. M. Rao, P. C. Eklund, and R. C. Haddon, *Science* **282**, 95 (1998).

¹⁹J. Sherman, *Spectrochim. Acta* **7**, 283 (1955).

²⁰N. B. Colthup, L. H. Daly, and S. E. Wiberly, *Introduction to Infrared and Raman Spectroscopy* (Academic, Boston, 1990), p. 240.

²¹M. J. Frisch, G. W. Trucks, H. B. Schlegel *et al.*, GAUSSIAN 03, Revision C.02, Gaussian, Inc., Wallingford, CT, 2004.